Proc. Natl. Acad. Sci. USA
Vol. 92, pp. 4686–4690, May 1995
Biochemistry

A secondary-structure model for the self-cleaving region of *Neurospora* VS RNA

(ribozyme/RNA catalysis/mitochondria/plasmid)

TARA L. BEATTIE, JOAN E. OLIVE, AND RICHARD A. COLLINS

Canadian Institute for Advanced Research Program in Evolutionary Biology, Department of Molecular and Medical Genetics, University of Toronto, Toronto, ON Canada M5S 1A8

Communicated by Olke C. Uhlenbeck, University of Colorado, Boulder, CO, December 19, 1994

ABSTRACT **_Neurospora_ VS RNA performs an RNA-mediated self-cleavage reaction whose products contain 2′,3′-cyclic phosphate and 5′-hydroxyl termini. This reaction is similar to those of hammerhead, hairpin, and hepatitis δ virus ribozymes; however, VS RNA is not similar in sequence to these other self-cleaving motifs. Here we propose a model for the secondary structure of the self-cleaving region of VS RNA, supported by site-directed mutagenesis and chemical modification structure probing data. The secondary structure of VS RNA is distinct from those of the other naturally occurring RNA self-cleaving domains. In addition to a unique secondary structure, several Mg-dependent interactions occur during the folding of VS RNA into its active tertiary conformation.**

Three naturally occurring RNA secondary structural motifs, the hammerhead (1), hairpin (2, 3), and hepatitis δ virus (for review, see ref. 4), have been found that perform RNA self-cleavage reactions whose products contain 2′,3′-cyclic phosphate and 5′-hydroxyl termini. These ribozymes are present in satellite RNAs of plant or animal viruses, where their role appears to be the production of monomer-length RNA from multimers synthesized during rolling-circle replication from RNA templates (5).

Neurospora VS RNA is transcribed from a plasmid DNA that is found in the mitochondria of several natural isolates of *Neurospora*. It is also a satellite RNA, in this case of a larger nonhomologous plasmid that encodes a reverse transcriptase (6, 7). Even though VS RNA is present at high concentrations, comparable to those of the mitochondrial rRNAs, no phenotype attributable to the plasmid has been observed. VS RNA performs the same type of RNA self-cleavage reaction as the other satellite RNAs but shows no sequence similarities, suggesting that it contains another ribozyme motif (6, 8). Here we propose a model for the secondary structure of the self-cleaving region of VS RNA. The model is supported and distinguished from alternative structures by site-directed mutagenesis and chemical modification structure-probing data.

MATERIALS AND METHODS

Clones and Site-Directed Mutagenesis. Clone G11 has been described (8) and contains bases 617–881 of VS RNA in vector pTZ19R. Mutations were made in clone G11 or ΔG11 (from which the *Sca* I, *Ava* I, and *Acy* I sites in the vector had been destroyed to facilitate future subcloning by retaining only a unique site for each enzyme within the VS sequence). Substitutions on the 5′ or 3′ side of a helix were made by oligonucleotide-directed mutagenesis (9); compensatory mutants were also made this way unless a unique restriction site separated the 5′ and 3′ mutations, in which case recombinant DNA techniques were used to combine the two mutations into a single clone. Usually two isolates of each mutant were identified and sequenced from the T7 promoter to the *Ssp* I site, which was the 3′ end of the run-off transcripts used to measure cleavage rates.

Measurement of Self-Cleavage Rates. RNAs were synthesized by T7 transcription from plasmid templates linearized with *Ssp* I (VS nt 783). Uncleaved precursor RNAs were obtained from wild type and active mutants by using decreased Mg concentrations during transcription (10). RNAs (≈50 nM) were dissolved in water, preincubated at 37°C, and mixed with 0.25 vol of 200 mM Tris·HCl, pH 8.0/250 mM KCl/10 mM spermidine/50 mM $MgCl_2$. Aliquots were removed at various times, and the precursor and product RNAs were separated by electrophoresis and quantitated by using a PhosphorImager as described (10). First-order self-cleavage rates were determined from the slopes of plots of the fraction of uncleaved RNA vs. time.

Chemical Structure Probing. RNAs were synthesized by T7 transcription from plasmid templates linearized with *Ssp* I or *Bam*HI (in the vector multiple cloning site). To obtain maximal yield of the downstream cleavage product, denoted G11/*Ssp*D or G11/*Bam*D, transcription was carried out for 1 h at 37°C, the template was inactivated with DNase I, and the concentration of $MgCl_2$ was increased to 15 mM for a further 15-min incubation. RNAs were purified from 8 M urea/4% polyacrylamide gels by elution in water, filtered through a 0.45-μm (pore size) cellulose acetate membrane, precipitated with ethanol, and dissolved in water. For subsequent diethyl pyrocarbonate (DEPC) modification, RNAs were labeled at the 3′ end by using 5′-[^{32}P]pCp and RNA ligase (11).

RNAs were modified with DEPC, dimethyl sulfate (DMS), kethoxal (KE), or 1-cyclohexyl-3-(2-morpholinoethyl)carbodiimide metho-*p*-toluenesulfonate (CMCT) as described (12–15), except for slight empirically determined adjustments to the concentrations of the modifying reagents. Modifications were performed under the following three conditions: (*i*) denaturing (200 mM Hepes, pH 8.0/1 mM EDTA at 90°C), (*ii*) semidenaturing (200 mM Hepes, pH 8.0/1 mM EDTA at 37°C), and (*iii*) native (200 mM Hepes, pH 8.0/50 mM KCl/10 mM $MgCl_2$ at 37°C) (15). The Hepes buffer was adjusted to pH 8.0 at 25°C with NaOH. For the CMCT reactions, Hepes was replaced with 50 mM sodium borate (pH 8.0) in some experiments.

For unlabeled RNAs modified at Watson–Crick pairing positions, sites of modification were determined by reverse transcription using primer extension (14, 16). Primer 1923 is complementary to nt 783–767 (for G11/*Ssp*D); primer 3357 is complementary to nt 827–811 (for G11/*Bam*D). End-labeled RNAs modified with DEPC were cleaved with aniline at the sites of modification (17).

The publication costs of this article were defrayed in part by page charge payment. This article must therefore be hereby marked "*advertisement*" in accordance with 18 U.S.C. §1734 solely to indicate this fact.

Abbreviations: DEPC, diethyl pyrocarbonate; DMS, dimethyl sulfate; KE, kethoxal; CMCT, 1-cyclohexyl-3-(2-morpholinoethyl)carbodiimide metho-*p*-toluenesulfonate.

RESULTS

As with other satellite RNAs, only a fraction of VS RNA is required for self-cleavage *in vitro* (8). For structure determination, we chose the region of VS RNA transcribed from clone G11 (ref. 10; Fig. 1*A*) because (*i*) it is only a few nucleotides longer than the minimal self-cleaving RNA, (*ii*) it can be conveniently synthesized in good yield by T7 RNA polymerase transcription, and (*iii*) its cleavage properties have been characterized.

Like hepatitis δ virus (18) and hairpin (19) ribozymes, there is little informative comparative sequence data available to assist in constructing structural models for VS RNA (ref. 8 and unpublished data). As an alternative starting point for structure prediction, we used the MFOLD program (version 2) of Zuker and collaborators (20–22) to obtain structural models that ranged from the folding predicted to be most stable to suboptimal foldings 10% less stable than the lowest free energy structure. Foldings within this range of free energy have been found to predict the majority of helices in other RNAs (22). We evaluated foldings of G11 pre-RNA (with and without the preceding vector nucleotides) and the minimal self-cleaving region of VS RNA (nt 620–773). Similar families of structures were found for all RNAs. The models differ in the number or length of helices and/or the predicted pairing partner for a given region of the sequence. Some representative alternative foldings are shown in Fig. 1.

Site-Directed Mutagenesis. To assess the relevance of the predicted structures to the cleavage activity of VS RNA, we constructed site-directed base substitution mutants. These mutants would be expected to disrupt a helix by changing one or more bases on the 5′ or 3′ side of a putative helix. Compensatory mutations that would restore a helix, but using a different base pair, were also constructed. Self-cleavage rates were measured for wild-type, the 5′ and 3′ mutants, and the compensatory mutant, denoted 5′3′. The data for representative mutants are shown in Table 1 and selected data are presented graphically in Fig. 1. Of the models we evaluated, that shown in Fig. 1*A* was by far the most consistent with the data from the cleavage activity of all of the mutants.

In general, mutations on the 5′ or 3′ side of predicted helices II–VI inactivated the ribozyme or decreased activity well below that of the wild-type sequence. Most compensatory substitutions restored activity to about that of wild type. Several of the compensatory substitutions, especially those involved in helices II and III, support only the structure shown in Fig. 1*A* and are not consistent with the alternative models in Fig. 1*B*. Given the formation of helices II–VI, the most reasonable folding of the remaining 5′ nucleotides would be the formation of helix I. These data show that regions of helices II–VI perform roles that are not sequence-specific but are presumably involved in proper folding of the RNA.

At some positions activity could not be restored by the compensatory substitutions attempted, even though restoration was possible at other positions in the same helix. This was especially common at predicted base pairs adjacent to natural disruptions in a helix, such as the unpaired adenosines at positions 652 and 718 (Table 1, helices IIc and IIIc, and data not shown). Deletion of either unpaired adenosine also decreased activity, severely so for A652. These observations

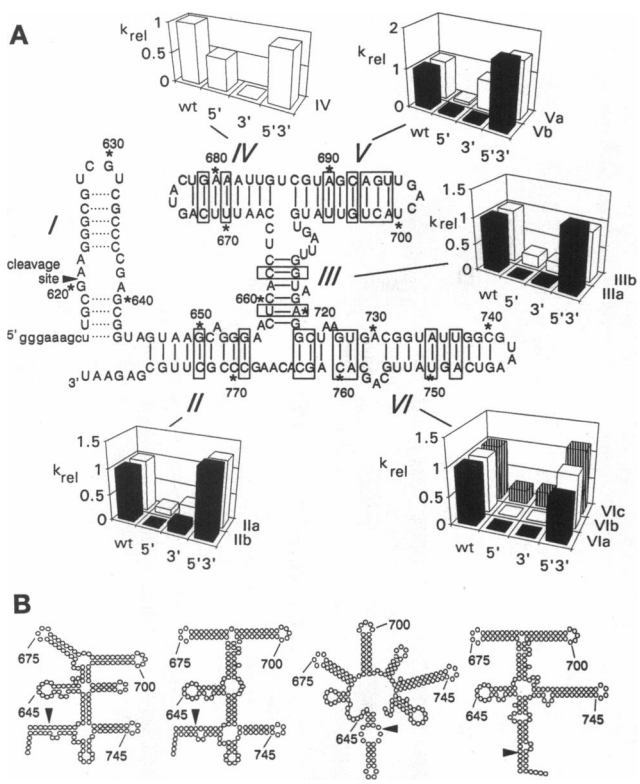

FIG. 1. Model of the secondary structure of G11 pre-RNA. (*A*) VS and vector nucleotides are in upper- and lowercase type, respectively. Bases are numbered as in ref. 6. Helices are indicated by Roman numerals. Boxes indicate positions in a helix where disruption of a base pair(s) eliminates or reduces activity and compensatory substitution restores activity. The cleavage rates of substitution mutants on the 5′ or 3′ sides of a helix and the compensatory substitutions (denoted 5′3′) are plotted relative to wild type (k_{rel}) (see Table 1 for details of the mutations). (*B*) Representatives of the major classes of alternative foldings predicted by MFOLD. The position of the self-cleavage site is indicated by the arrowhead. Vector nucleotides are not included.

Table 1. Effect of mutations in helices on the rate of self-cleavage

Helix	Mutation	k_{rel}	Helix	Mutation	k_{rel}
—	G11 wild type	1.00	IIId	5′ C665G	0.01
Ia	5′ G624C/G625C	0.02		3′ G711C	F
	3′ C634G/C635G	0.64		5′3′	0.01
	5′3′	<0.01	IV	5′ U670A/C672G	0.54
Ib	5′ C626G	1.21		3′ G679C/A681U	<0.01
	3′ G633C	0.74		5′3′	0.88
	5′3′	0.31	Va	5′ A690U/C692G	0.07
Ic	5′ G627C	0.64		3′ G704C/U706A	0.78
	3′ C632G	<0.01		5′3′	1.48
	5′3′	<0.01	Vb	5′ U695G	0.06
IIa	5′ G650C	0.12		3′ A701C	0.04
	3′ C773G	0.29		5′3′	1.67
	5′3′	1.27	Vc	5′ A693U/G694C	ND
IIb	5′ G655C	<0.01		3′ C702G/U703A	ND
	3′ C769G	0.18		5′3′	0.31
	5′3′	1.32	VIa	5′ G722C/C723G	<0.01
IIc	5′ G653C	<0.01		3′ G762C/C763G	<0.01
	3′ C771G	<0.01		5′3′	0.75
	5′3′	0.09	VIb	5′ G727C/U728A	<0.01
IIIa	5′ U659A	<0.01		3′ A759U/C760G	<0.01
	3′ A720U	0.05		5′3′	0.94
	5′3′	1.19	VIc	5′ A735U/U737A	0.25
IIIb	5′ C662G	0.23		3′ A748U/U750A	0.28
	3′ G716C	0.21		5′3′	1.15
	5′3′	0.94	652ΔA		<0.01
IIIc	5′ A661U/C662G	0.06	A652G		<0.01
	3′ G716C/U717A	0.02	718ΔA		0.15
	5′3′	0.08			

k_{rel} is the rate constant of the mutant divided by the rate constant of wild-type G11. The rate constant for G11 varied from ≈0.06 to 0.08 min^{-1}. F, cleavage rate not measured accurately but was similar to wild type. Vb mutants were made in a variant of G11 that contained two different base pairs in helix V (mutant Vc); rates were normalized by using mutant Vc as the relevant wild type. ND, cleavage rate not determined.

suggest that specific local structures may be especially important in these areas or that some of these bases may be involved in alternative and/or additional interactions.

The structure and sequence requirements of helix I appear to be more complex than implied by the model in Fig. 1*A*. Although several base substitutions decreased activity severely (mutants Ia5′, Ic3′, and others not shown), other mutations that might be expected to have an equally disruptive effect on the helix (mutants Ia3′, Ib3′, and Ic5′) decreased activity only slightly. We have not found any positions at which the compensatory substitutions that we have tried restored activity much above the level of the individual mutants. Nonetheless, the existence and stability of helix I are supported by chemical structure probing and difficulties in sequencing this region (see below). Thus, these observations suggest that certain bases in helix I may be involved in alternative secondary structures or tertiary interactions that are crucial for activity.

Chemical Modification Structure Probing. To obtain independent information about the structure of G11 RNA, we performed chemical modifications under conditions that allow self-cleavage—i.e., in the presence of Mg (native conditions) or in the absence of Mg (semidenaturing conditions). Because G11 pre-RNA self-cleaves under native conditions, this would lead to a mixture of RNAs that might complicate interpretation of the modification data. To avoid this problem, the structure probing shown here was done with G11D, the downstream cleavage product. G11D and the minimal self-cleaving RNA differ at their 5′ ends by only a single nucleotide, whose identity is not critical (8). DEPC modification of G11 pre-RNA under semidenaturing conditions (data not shown) supports the assumption that G11D remains in essentially the same secondary structure as the self-cleaving RNA. These experiments are also consistent with the formation of the helix upstream of the cleavage site shown in Fig. 1*A*; however, previous deletion analysis has shown that this helix is not required for self-cleavage (8).

Fig. 2 *A* and *B* shows the results of DEPC modification of G11D. DEPC is a very useful reagent for determining both secondary and tertiary interactions because the N7 position of adenosine is protected from modification if the base is either stacked in a helix or involved in a long-range interaction (15). With the exception of the two adenosines at the 5′ end, which cannot be resolved from full-length RNA, all of the adenosines predicted to be unpaired in the model shown in Fig. 1*A* were modified by DEPC under semidenaturing conditions. One of these (A764) was modified only weakly, suggesting it may be stacked or involved in a non-Watson–Crick interaction, even in the absence of Mg. Some of the modifications were enhanced under semidenaturing conditions, suggesting that the local environment allows the residue to be more reactive to the modifying reagent, compared to the denaturing reaction. Seventeen of the 19 adenosines predicted to be in helices were protected. The exceptions were A701 and A761, which are at the ends of helices and might, therefore, be expected to be accessible to DEPC (23). The DEPC modification data (Fig. 3) provide strong support for this secondary structure model and are not consistent with alternative models (see Fig. 1*B*).

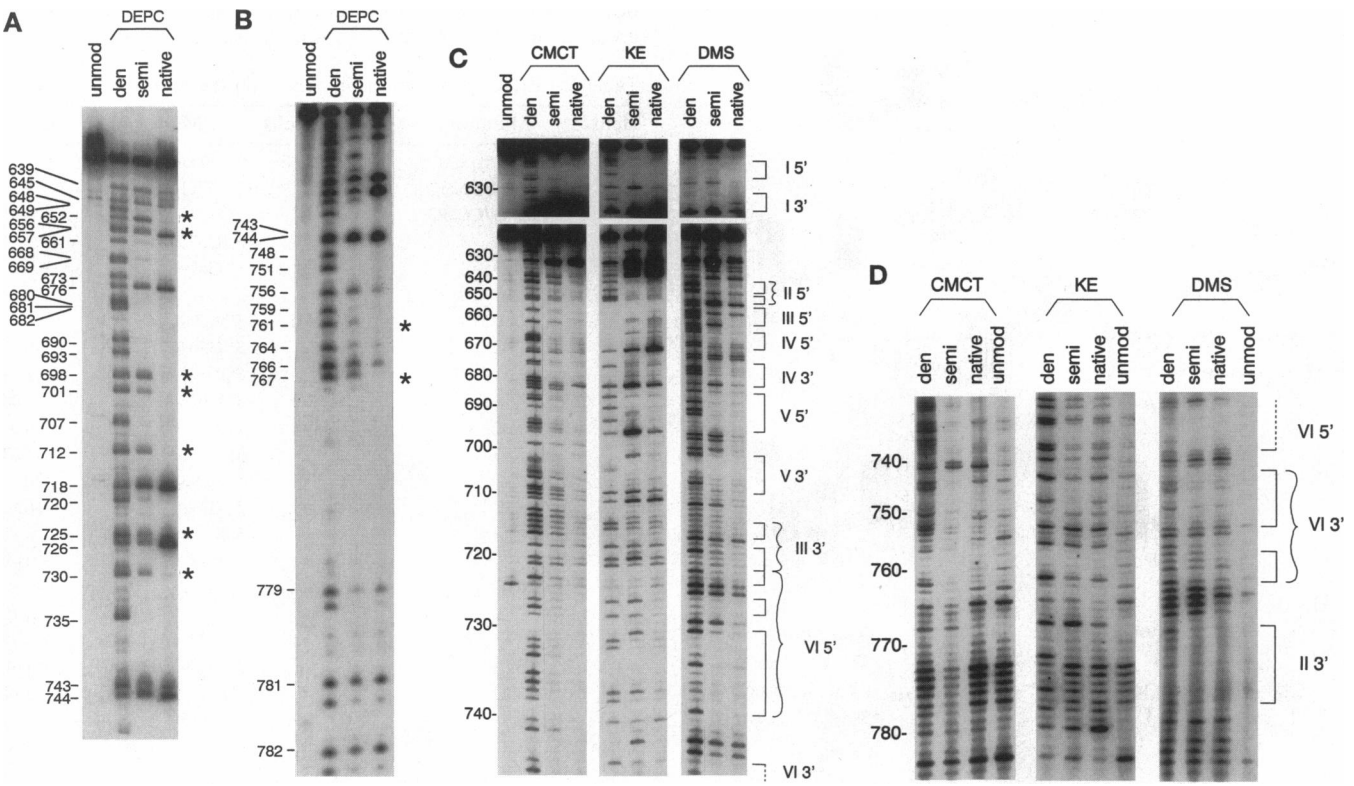

FIG. 2. Chemical modification structure probing. Modifications were performed under denaturing (den), semidenaturing (semi), or native conditions. Control samples that were not exposed to the modifying reagents are included (unmod). (*A* and *B*) Modification of adenosine N7. G11/*Ssp*D RNA (3′-end labeled) was modified with DEPC. Sites of modification were detected by cleavage with aniline, electrophoresis on 8.3 M urea/8% (*A*) or 22% (*B*) polyacrylamide gels, and autoradiography. Bases that are protected only under native conditions are indicated by *. (*C* and *D*) Modification of Watson–Crick pairing positions. G11/*Ssp*D RNA (*C*) or G11/*Bam*D RNA (*D*) was modified with CMCT, KE, or DMS; sites of modification were detected by reverse transcription with primers 1923 (*C*) or 3357 (*D*) on 8.3 M urea/8% polyacrylamide gels followed by autoradiography. In *C* different exposures of a single gel were spliced together to account for different loadings. Bands in the KE semidenaturing and native lanes that do not correspond to guanosine residues were not reproducible on other gels. In the upper portion of *C*, the samples were separated on a 8.3 M urea/6% polyacrylamide gel to obtain improved resolution of helix I. Bases involved in the formation of the 5′ or 3′ sides of the helices in Fig. 1 are indicated by the square brackets on the right. Helices with single-stranded disruptions (i.e., internal loops or bulged nucleotides) are grouped together with braces.

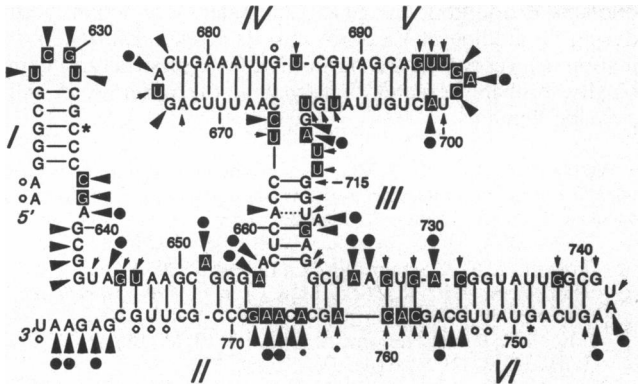

FIG. 3. Summary of chemical reactivities. The degree of modification under semidenaturing conditions is classified as strong (large symbols) or weak (small symbols) as estimated from autoradiographic band intensities (Fig. 2 and data not shown). Modification at Watson–Crick base-pairing positions or A–N7 positions are represented by arrowheads or circles, respectively. For simplicity, a single symbol is used for KE and CMCT modification of G-N1. Bases whose reactivities could not be determined due to stops in all lanes or that are in close proximity to dark bands are indicated by open circles. Bases that are more protected from chemical modification under native conditions than under semidenaturing conditions are indicated by solid boxes; those that are more reactive are indicated by *.

Under native conditions, nine additional adenosines were protected from DEPC modification (indicated by asterisks in Fig. 2 *A* and *B* and summarized in Fig. 3). These bases are candidates for non-Watson–Crick base pairs, interactions involving the N7 position and another base, a sugar, or a Mg^{2+}, or local structure changes that protect the N7, possibly by stacking on an adjacent base. The additional protections observed under native conditions are distributed throughout the RNA, suggesting that formation of higher-order structure involves multiple new interactions.

In addition to DEPC modification, we also monitored Watson–Crick pairing positions of each base by modification with KE (at G-N1 and G-N2), DMS (at A-N1 and C-N3), or CMCT (at U-N3 and G-N1) followed by reverse transcription. Modification of ≈40 nt at the 3′ end of G11/*Ssp*D could not be determined because this region contained or was too close to the primer hybridization site. To investigate this region, a longer RNA, G11/*Bam*D and a distal primer were used. In the region where modification of both the *Ssp* and *Bam* transcripts could be evaluated, they showed essentially the same modification patterns (Fig. 2*D* and data not shown).

As with DEPC modification, bases predicted to be in single-stranded regions were modified under semidenaturing conditions (Fig. 2 *C* and *D* and summarized in Fig. 3). Some bases at the ends of helices or adjacent to natural disruptions in a helix (e.g., the unpaired adenosines at positions 652 and 718 or the internal loops in helix VI) were also modified. Similar observations have been made with other RNAs (13, 15) and may reflect structural dynamics, such as transient breaking and reforming of hydrogen bonds or noncanonical local structure.

Most of the bases predicted to form the 5′ or 3′ sides of helices I–VI (indicated by the square brackets in Fig. 2 *C* and *D*) were protected to various degrees from modification. However, in contrast to the clear identification of protected bases when DEPC modification and aniline cleavage of end-labeled RNA was used (Fig. 2 *A* and *B*), faint bands suggestive of base modification were common when primer extension was used to detect modification of the Watson–Crick pairing positions. The modification of bases that might be expected to be protected by hydrogen bonding within helices suggests that the structure is sufficiently dynamic during the time of these modification reactions to allow even base-paired positions to be reactive with certain modifying reagents (13). These reactions were performed at 37°C to approximate the conditions used for measuring self-cleavage activity, rather than at a lower temperature that might have favored helix stability. The alternative explanation that some of the RNA was in other stable conformations seems less likely because modification with DEPC (Fig. 2 *A* and *B*) gave no indication of reactivity of bases predicted to be in helices.

The only strong modification of a base predicted to be in a helix occurred with DMS at N1 of A661. This suggests that A661 is not in a stable Watson–Crick pair. Also, the N7 of this base is protected from DEPC modification, raising the possibility that A661 is involved in a noncanonical interaction, possibly a reverse-Hoogsteen pair with U717. With the exception of A661, the extent of modification of bases predicted to be in helices was usually much less than for single-stranded bases. Thus, the DMS, KE, and CMCT modifications of Watson–Crick pairing positions and the DEPC modifications of adenosine N7 positions support the proposed secondary-structure model.

Under native conditions, several additional bases were protected from DMS, KE, and/or CMCT (Fig. 2 *C* and *D* and summarized in Fig. 3). Most of these are located at the junctions of helices II/III/VI (A656 and A767) and III/IV/V (U664, C665, U686, A712, U713, and U714), in the internal loops in helix VI (A725 and A730), and in the loops at the ends of helices I (U628, C629, G630, and U631) and V (U696, G697, A698, C699, and A701). These data extend the conclusions from DEPC modification and indicate that a large number of additional interactions form in the presence of Mg. One position, C634, which was protected under semidenaturing conditions, was accessible to DMS under native conditions, suggesting that a conformational change may occur in helix I in the presence of Mg.

DISCUSSION

We have constructed a model for the secondary structure of the G11 ribozyme that contains the minimal contiguous region of VS RNA required for self-cleavage. In five of the six helices proposed in the model, site-directed base substitution mutations that disrupt the helix decrease or eliminate activity. Compensatory substitutions restore activity, usually to wild-type level or even greater. These data provide strong support for a sequence-independent, presumably structural, role for portions of these five helices.

The formation of all six helices in the secondary structure model is supported by chemical modification under semidenaturing conditions (i.e., in the absence of Mg). Most of the chemical modification structure probing was performed on the downstream self-cleavage product, which differs from an active RNA by lacking only a single nucleotide upstream of the cleavage site. The observation that the chemical modification data are consistent with the same model deduced from the results of site-directed mutagenesis supports the assumptions that precursor RNA and the downstream cleavage product have similar secondary structures. Since these two approaches support the same model and are inconsistent with the alternative models examined, we expect that the model in Fig. 1*A* is a good representation of the actual secondary structure.

There are few opportunities for additional Watson–Crick pairing beyond those that form in semidenaturing conditions (Fig. 3). This adds support to the proposal deduced from observations with other RNAs that secondary structure forms in the absence of Mg and before tertiary structure (24–26). Nonetheless, under native conditions (i.e., in the presence of Mg), a large number of additional bases are protected from chemical modification (Fig. 3). If the secondary structure remains intact, these bases are likely to be involved in tertiary

interactions or noncanonical local structure. The distribution of these protected bases throughout the RNA suggests that the active tertiary structure of the G11 ribozyme is rather complex and involves multiple interactions.

Several observations suggest that the formation of the active structure is more complicated than implied above. While site-directed mutants of helices II–VI indicate that portions of these helices play a sequence-independent structural role, mutants in helix I show a more complex pattern. Mutations at certain positions in helix I inactivated the ribozyme but compensatory substitutions did not restore activity. Also, C634, which is protected from DMS modification under semi-denaturing conditions and is base-paired within helix I, becomes accessible under native conditions. Thus, these observations suggest that conformational changes may occur during formation of the active structure of VS RNA under native conditions.

Our model predicts that VS RNA contains some structural features found or predicted in other RNAs. The GUAA tetraloop capping helix VI is an example of a GNRA loop that is common in rRNAs (27) and contains internal hydrogen bond and stacking interactions that stabilize the loop structure (28, 29). We were surprised to find that the N7 position of the last adenosine in this loop was very accessible to DEPC modification, because the structure of very similar loops (GAAA and GCAA), as determined by NMR, suggested stacking of the last two adenosines and a hydrogen bond between the N7 of the last adenosine and the exocyclic amino group of the guanosine. The chemical modification data suggest either that the intra-loop structure does not form in VS RNA or that the loop is sufficiently dynamic to allow reactivity with DEPC.

G·A base pairs at the ends of helices or in internal loops are another recurring noncanonical interaction in RNAs (30, 31). In the recently determined hammerhead crystal structure, adjacent G·A pairs have been found to be a metal binding site (32). Our model of VS RNA secondary structure suggests the possibility of G·A base pairs within the internal loops of helices I and VI and at both ends of helix II. Indeed, several of these bases (G638, A656, A730, and G768) are protected from chemical modification under native conditions (Figs. 2*A* and 3), indicating that they are not simply single-stranded, as shown in our model. Also, site-directed mutagenesis of one these positions, A622, which is too near the 5′ end of the RNA to be resolved in Fig. 2, shows that it is essential for activity (J.E.O. and R.A.C., unpublished data). These modification and mutational data are consistent with the formation of noncanonical interactions at the ends of some of these helices.

The secondary structure of VS RNA is different from the hammerhead and hairpin ribozymes in that, although a short helix upstream of the site of cleavage could form in VS RNA, it is not required for activity (8) as it is in these two other ribozymes (1, 3). Also, G11 RNA does not contain the set of bases known to be important for activity of hammerhead (5) or hairpin (3, 33) ribozymes. Like VS RNA, the hepatitis δ virus ribozyme (4) requires only a single nucleotide upstream of the cleavage site, and a GC-rich helix is found downstream of the cleavage site in both ribozymes. Beyond these similarities, however, the secondary structures have nothing obvious in common.

In conclusion, the secondary structure of the self-cleaving region of VS RNA is different from other RNA self-cleaving domains. In addition, several Mg-dependent interactions occur during the folding of VS RNA into its active tertiary conformation, suggesting that it has a high level of structural complexity, probably greater than that of the other RNA self-cleaving domains.

We thank M. Dizonno, N. MacPherson, and G. Kissin for constructing some of the mutants. This work was supported by a grant from the Medical Research Council of Canada.

1. Forster, A. C. & Symons, R. H. (1987) *Cell* **50,** 9–16.
2. Hampel, A., Tritz, R., Hicks, M. & Cruz, P. (1990) *Nucleic Acids Res.* **18,** 299–304.
3. Joseph, S., Berzal-Herranz, A., Chowrira, B. M., Butcher, S. E. & Burke, J. M. (1993) *Genes Dev.* **7,** 130–138.
4. Been, M. D. (1994) *Trends Biochem. Sci.* **19,** 251–256.
5. Symons, R. H. (1992) *Annu. Rev. Biochem.* **61,** 641–671.
6. Saville, B. J. & Collins, R. A. (1990) *Cell* **61,** 685–696.
7. Kennel, J. C., Saville, B. J., Mohr, S., Kuiper, M. T. R., Sabourin, J. R., Collins, R. A. & Lambowitz, A. M. (1995) *Genes Dev.* **9,** 294–303.
8. Guo, H. C.-T., De Abreu, D. M., Tillier, E. R. M., Saville, B. J., Olive, J. E. & Collins, R. A. (1993) *J. Mol. Biol.* **232,** 351–361.
9. Kunkel, T. T., Roberts, J. D. & Zakour, R. A. (1987) *Methods Enzymol.* **154,** 367–382.
10. Collins, R. A. & Olive, J. E. (1993) *Biochemistry* **32,** 2795–2799.
11. Bruce, A. G. & Uhlenbeck, O. C. (1978) *Nucleic Acids Res.* **5,** 3665–3677.
12. Peattie, D. & Gilbert, W. (1980) *Proc. Natl. Acad. Sci. USA* **77,** 4679–4682.
13. Krol, A. & Carbon, P. (1989) *Methods Enzymol.* **180,** 212–227.
14. Stern, S., Changchein, L.-M., Craven, G. R. & Noller, H. F. (1988) *J. Mol. Biol.* **200,** 291–299.
15. Ehresmann, C., Baudin, F., Mougil, M., Romby, P., Ebel, J.-P. & Ehresmann, B. (1987) *Nucleic Acids Res.* **15,** 9109–9128.
16. Inoue, T. & Cech, T. R. (1985) *Proc. Natl. Acad. Sci. USA* **82,** 648–652.
17. Peattie, D. A. (1979) *Proc. Natl. Acad. Sci. USA* **76,** 1760–1764.
18. Rosenstein, S. P. & Been, M. (1991) *Nucleic Acids Res.* **19,** 5409–5416.
19. Rubino, L., Tousignant, M. E., Steger, G. & Kaper, J. M. (1990) *J. Gen. Virol.* **71,** 1897–1903.
20. Zuker, M. (1989) *Science* **244,** 48–52.
21. Jaeger, J. A., Turner, D. H. & Zuker, M. (1990) *Methods Enzymol.* **183,** 281–306.
22. Jaeger, J. A., Turner, D. H. & Zuker, M. (1989) *Proc. Natl. Acad. Sci. USA* **86,** 7706–7710.
23. Weeks, K. M. & Crothers, D. M. (1993) *Science* **261,** 1574–1577.
24. Crothers, D. M., Cole, P. E., Hilbers, C. W. & Shulman, R. G. (1974) *J. Mol. Biol.* **87,** 63–88.
25. Jaeger, J., Zuker, M. & Turner, D. H. (1990) *Biochemistry* **29,** 10147–10158.
26. Banerjee, A. R., Jaeger, J. A. & Turner, D. H. (1993) *Biochemistry* **32,** 153–163.
27. Woese, C. R., Winker, S. & Gutell, R. R. (1990) *Proc. Natl. Acad. Sci. USA* **87,** 8467–8471.
28. Heus, H. & Pardi, A. (1991) *Science* **253,** 191–194.
29. SantaLucia, J., Jr., Kierzek, R. & Turner, D. H. (1992) *Science* **256,** 217–219.
30. SantaLucia, J., Jr., Kierzek, R. & Turner, D. H. (1990) *Biochemistry* **29,** 8813–8819.
31. Gautheret, D., Konings, D. & Gutell, R. R. (1994) *J. Mol. Biol.* **242,** 1–8.
32. Pley, H. W., Flaherty, K. M. & McKay, D. B. (1994) *Nature (London)* **372,** 68–74.
33. Berzal-Herranz, A., Joseph, S., Chowrira, B. M., Butcher, S. E. & Burke, J. M. (1993) *EMBO J.* **12,** 2567–2574.